I&EC research
Industrial & Engineering Chemistry Research

Article

pubs.acs.org/IECR

A Perturbed-Chain SAFT Equation of State Applied to Mixtures of Short- and Long-Chain *n*-Alkanes

Khashayar Nasrifar*

Chemical Engineering Department, Universiti Teknologi Petronas, Tronoh 31750, Perak, Malaysia

Supporting Information

ABSTRACT: A simplified hard-chain dimer theory is employed with perturbed-chain statistical associating fluid theory (PC-SAFT) in calculating the vapor pressures and saturated liquid volumes of pure *n*-alkanes from methane to *n*-eicosane. Compared to the original PC-SAFT, the developed model is in better agreement with the experimental vapor pressures and saturated liquid volumes of *n*-alkanes along the vapor−liquid coexistence curve and the critical properties from *n*-butane toward longer *n*-alkanes. Predicting the vapor−liquid equilibria (VLE) of binary mixtures containing methane and a long-chain *n*-alkane, the new model describes the mixtures more accurately than PC-SAFT. With no binary interaction parameter, the model adequately describes the experimental VLE data, in particular, near the critical points. In the prediction of the VLE of mixtures containing ethane, propane, *n*-hexane, and a long-chain *n*-alkane, the differences between the two models become less appreciable.

INTRODUCTION

Equilibrium features of petroleum fluids can also be found in phase equilibria of short and long *n*-alkane mixtures. In particular, hyperbaric reservoirs, where the fluids coexist at high pressure and high temperature, are composed of short- and long-chain hydrocarbons.[1] The difference in size causes asymmetry, thus making phase equilibrium calculations inaccurate, especially when a cubic equation of state is used.[2,3] Equations of state with a theoretical basis, however, have been fruitful in describing the phase equilibria of short- and long-chain hydrocarbon mixtures.[4−6] In particular, statistical associating fluid theory (SAFT)[7,8] has gained much interest because of its accuracy in describing the phase equilibria of chain molecules and polymers.[9,10]

Since its conception, the SAFT approach has been modified to accurately describe the phase equilibria of different mixtures. For practical purposes, the SAFT version of Huang and Radosz[11,12] gained particular interest for almost a decade. Thereafter, new approaches in SAFT modeling emerged. Vega and co-workers developed soft-SAFT.[13−15] These investigators employed crossover theory to study the behavior of *n*-alkane−*n*-alkane mixtures away from and close to the critical points.[16] Applying White's idea,[17,18] the authors quantitatively described the phase equilibria of the systems methane + *n*-pentane, methane + *n*-hexane, ethane + *n*-decane, and ethane + *n*-eicosane. SAFT for potentials of variable range (SAFT-VR) is another fruitful approach.[19] Rescaling the SAFT-VR parameters by experimental critical points, McCabe et al.[20] succeeded in describing the vapor−liquid equilibria of the systems containing *n*-butane with other *n*-alkanes. Despite significant improvement near the critical points, poor agreement was obtained at lower pressures, especially at lower temperatures. Circumventing this shortcoming with SAFT-VR, Sun et al.[21] applied the proposed approach of Kiselev[22,23] to predict the phase equilibria of short *n*-alkanes away from and close to the critical point. Introducing a new dispersion term,[24] Gross and Sadowski[25] developed an improved version of SAFT called perturbed-chain SAFT (PC-SAFT). Using thermodynamic perturbation theory (TPT) for dimer molecules,[26] Dominik et al.[27] developed a new SAFT approach called perturbed-chain dimer SAFT (PC-SAFT-D). PC-SAFT-D markedly described the phase equilibria of hydrocarbon mixtures without applying binary interaction parameters. Although based on a mean field theory, PC-SAFT-D accurately described the vapor−liquid equilibria of systems containing short- and long-chain *n*-alkane molecules far from and near the critical points. Despite its merits, PC-SAFT-D suffers from a major drawback; that is, PC-SAFT-D cannot be applied to spherical molecules or molecules with less than two equivalent segment numbers. Compared to the original PC-SAFT, the dimer version also looks more complicated.

Indeed, the difficulty originated from TPT dimer theory (TPT-D), which was independently developed by Ghonasgi and Chapman[28] and Chang and Sandler.[29] The authors considered hard-dimers as building blocks of long-chain molecules. Consequently, the theory cannot be applied to hard-sphere molecules. Furthermore, the dimer theory takes advantage of the radial distribution function for hard-dimer molecules, which exceeds the complexity of the theory, especially for mixtures. TPT-D can be simplified using the hard-dimer radial distribution function developed by Nasrifar and Bolland.[30] The hard-dimer radial distribution function of Nasrifar and Bolland[30] is simply expressed in terms of radial distribution function of hard-spheres by

$$\mathrm{d}\ln g^{\mathrm{hd}}(\sigma) = S_{\mathrm{R}}\,\mathrm{d}\ln g^{\mathrm{hs}}(\sigma) \tag{1}$$

where g is the radial distribution function at contact, σ is the hard-sphere diameter, hd represents the hard-dimer, hs represents the hard-sphere, and S_{R} is the ratio of the surface area of a hard dimer to the surface area of a hard-sphere with

Received: January 8, 2013
Revised: April 11, 2013
Accepted: April 19, 2013

   dx.doi.org/10.1021/ie400081a | *Ind. Eng. Chem. Res.* XXXX, XXX, XXX−XXX

the same volume as the hard-dimer. The numerical value of S_R is easily found to be $2^{1/3}$. The TPT-D can significantly be simplified if eq 1 is used for the radial distribution function of hard-dimers. The major problem with TPT-D was then fixed by setting eq 1 into TPT-D and shifting the constant 1.1150 to 1.[31] The modified TPT-D reads

$$Z^{hc} = 1 + m\left(\frac{4\eta - 2\eta^2}{(1-\eta)^3}\right) + \delta(1-m)\eta\frac{\partial \ln g^{hs}(\sigma)}{\partial \eta} \quad (2)$$

where Z is the compressibility factor, m is the segment number, η is the packing fraction, and δ is a constant equal to $(1 + 2^{1/3})/2$. If the parameter δ in eq 2 approaches 1, TPT will clearly be recovered. When eq 2 was compared to the original TPT-D in calculating the compressibility factor of hard-chain molecules, its accuracy was a bit less.[31] However, eq 2 can easily be extended to monomers as well as long-chain molecules.

This paper employs a model almost identical to the PC-SAFT approach to describe the critical and saturated properties of pure *n*-alkanes and the phase equilibria of systems containing short- and long-chain *n*-alkanes. Our aim is to maintain the characteristics of the PC-SAFT equation of state while improving its significance related to *n*-alkane chain length. Equation 2 is used to describe the repulsive behavior of chains as well as spherical molecules. The dispersion contribution is adapted from the original PC-SAFT equation.[25] The equation parameters are obtained from the fit of vapor pressures and saturated liquid volumes of *n*-alkanes from the triple point to the critical point. For the first few hydrocarbons, pressure−volume−temperature (PVT) data are also included as these species are often supercritical at reservoir conditions. Although no binary interaction parameter is used, the equation is applied to describe the phase equilibria of binary *n*-alkane mixtures near and far from the critical points. Compared to the original PC-SAFT, which uses TPT, the PC-SAFT approach in this work uses a simplified TPT-D and shows improvement in predicting pure component properties and certain vapor−liquid equilibria (VLE) of binary systems containing short- and long-chain *n*-alkanes.

PC-SAFT APPROACH

In this approach, the residual Helmholtz free energy of a fluid at the temperature and density of interest can be expressed by

$$a^{res} = a^{hc} + a^{disp} + a^{assoc} + a^{polar} \quad (3)$$

where $a^{res} = A^{res}/RT$ and A^{res} is the residual Helmholtz free energy. Equation 3 expresses that different interactions contribute to the residual Helmholtz free energy of a fluid, that is, hard-chain repulsion, dispersion, association, and polar interaction, respectively. This work entirely focuses on short- and long-chain *n*-alkanes. Then, the association[7,32−34] and polar contributions[35−39] to the Helmholtz free energy of hydrocarbons vanish. The hard-chain contribution to the residual Helmholtz free energy of chain molecules is expressed by

$$a^{hc} = a^{hs} + a^{chain} \quad (4)$$

where a^{hs} and a^{chain} stand for the Helmholtz free energy of hard-spheres and chain connectivity, which form the chain molecules. The hard-sphere contribution (a^{hs}) was defined independently by Boublik[40] and Mansoori et al.[41] as expressed by

$$a^{hs} = \frac{\bar{m}}{\zeta_0}\left[\frac{3\zeta_1\zeta_2}{1-\zeta_3} + \frac{\zeta_2^3}{\zeta_3(1-\zeta_3)^2} + \left(\frac{\zeta_2^3}{\zeta_3^2} - \zeta_0\right)\ln(1-\zeta_3)\right] \quad (5)$$

where

$$\zeta_n = \frac{\pi}{6}\rho\sum_i x_i m_i d_{ii}^n \quad \text{with} \quad n \in \{0, 1, 2, 3\} \quad (6)$$

and ρ is the number density, x_i is the mole fraction of component i, m_i is the number of segments for component i, and d_{ii} is the segment diameter. The parameter d_{ii} accounts for soft repulsion between segments. In terms of segment diameter (σ_{ii}) and the depth of square-well potential (ε_{ii}), the soft repulsion diameter is expressed by[42]

$$d_{ii}(T) = \sigma_{ii}\left[1 - 0.12\exp\left(-\frac{3\varepsilon_{ii}}{kT}\right)\right] \quad (7)$$

The chain connectivity contribution (a^{chain}) accounts for bond formations between the segments of a molecule. In most SAFT theories, monomer segments are the building blocks of chain formation. Chapman et al.[7] derived an expression of chain connectivity based on this premise and Wertheim's theory of association. The Chapman et al.[7] equation of chain connectivity is often used in the literature; however, it oversimplifies the bond formation process. In fact, bond formation in chain molecules is a sequential process, and the presence of previous bonds cannot be ignored in the formation of new bonds. Ghonasgi and Chapman[28] fixed this drawback by introducing dimer segments in the process of bond formation. The Ghonasgi and Chapman[28] chain connectivity term dramatically improved the previous chain connectivity term[7] at the expense of more complexity. However, a new shortcoming also emerged. The newly developed term was singular for molecules with less than two equivalent segment numbers. The latter was examined by Nasrifar,[31] and finally eq 2 was derived semiempirically. On the basis of eq 2, the chain connectivity contribution to the Helmholtz free energy of a chain molecule is derived as

$$a^{chain} = \delta\sum_i x_i(1-m_i)\ln[g_i^{hs}(d_{ii})] \quad (8)$$

where $\delta = (1 + 2^{1/3})/2$ and $g_i^{hs}(d_{ii})$ is the radial distribution function at contact for segments of component i in the hard-sphere system. Clearly, if δ approaches 1 in eq 8, the Chapman et al.[7] expression of chain connectivity will be recovered. In eq 8, $g_i^{hs}(d_{ii})$ is given by[41]

$$g_i^{hs}(d_{ii}) = \frac{1}{1-\zeta_3} + \left(\frac{d_{ii}}{2}\right)\frac{3\zeta_2}{(1-\zeta_3)^2} + \left(\frac{d_{ii}}{2}\right)^2\frac{2\zeta_2^2}{(1-\zeta_3)^3} \quad (9)$$

In the PC-SAFT approach, the dispersion contribution to the Helmholtz free energy is a second-order perturbation theory[25]

$$a^{disp} = a_1^{disp} + a_2^{disp} \quad (10)$$

For chain-like molecules, the parameters a_1^{disp} and a_2^{disp} have the forms

dx.doi.org/10.1021/ie400081a | Ind. Eng. Chem. Res. XXXX, XXX, XXX−XXX

$$a_1^{\text{disp}} = -2\pi\rho I_1 \sum_i \sum_j x_i x_j m_i m_j \left(\frac{\varepsilon_{ij}}{kT}\right)\sigma_{ij}^3 \tag{11}$$

$$a_2^{\text{disp}} = -\pi\rho I_2 \bar{m} C_1 \sum_i \sum_j x_i x_j m_i m_j \left(\frac{\varepsilon_{ij}}{kT}\right)^2 \sigma_{ij}^3 \tag{12}$$

where $\bar{m}$ is the mean segment number

$$\bar{m} = \sum_i x_i m_i \tag{13}$$

and C_1 is the compressibility of hard-chain fluid

$$C_1 = \left(1 + Z^{\text{hc}} + \rho\frac{\partial Z^{\text{hc}}}{\partial\rho}\right)^{-1} \tag{14}$$

In eq 14, Z^{hc} is the hard-chain compressibility factor. The values of Z^{hc} and its derivatives are evaluated from eq 2. Setting eq 2 into eq 14 yields

$$C_1 = \left(1 + \bar{m}\frac{8\eta - 2\eta^2}{(1-\eta)^4} + \delta\left(1 + \frac{0.2}{\bar{m}}\right) \times (1-\bar{m}) \times \frac{20\eta - 27\eta^2 + 12\eta^3 - 2\eta^4}{[(1-\eta)(2-\eta)]^2}\right)^{-1} \tag{15}$$

It must be pointed out that the impact of δ is appreciable on the value of C_1 and may not be ignored. The term $(1 + 0.2\bar{m})$ was inset empirically to augment parametrization of the new model near and far from the critical points, especially for short hydrocarbons. The value of 0.2 is arbitrary. A larger value would lead to a better description of vapor−liquid equilibria near and at the critical points. However, the accuracy of the model declines at lower pressures. The integrals I_1 and I_2 are functions of hard-chain site−site correlation function, chain length, and density. As the hard-chain site−site correlation functions are not accurate for long-chain molecules and the calculations were tedious, Gross and Sadowski[25] provided the following two approximations for I_1 and I_2:

$$I_1 = \sum_{i=0}^{6} a_i(\bar{m})\eta^i \tag{16}$$

$$I_2 = \sum_{i=0}^{6} b_i(\bar{m})\eta^i \tag{17}$$

The coefficients are provided by ref 25

$$a_i(\bar{m}) = a_{0i} + \left(\frac{\bar{m}-1}{\bar{m}}\right)a_{1i} + \left(\frac{\bar{m}-1}{\bar{m}}\right)\left(\frac{\bar{m}-2}{\bar{m}}\right)a_{2i} \tag{18}$$

$$b_i(\bar{m}) = b_{0i} + \left(\frac{\bar{m}-1}{\bar{m}}\right)b_{1i} + \left(\frac{\bar{m}-1}{\bar{m}}\right)\left(\frac{\bar{m}-2}{\bar{m}}\right)b_{2i} \tag{19}$$

where a_{0i}, a_{1i}, a_{2i}, b_{0i}, b_{1i}, and b_{2i} are constants. These constants were provided by Gross and Sadowski.[25]

For calculating ε_{ij} and σ_{ij}, conventional combining rules are employed

$$\varepsilon_{ij} = \sqrt{\varepsilon_{ii}\varepsilon_{jj}}(1 - k_{ij}) \tag{20}$$

$$\sigma_{ij} = \frac{\sigma_{ii} + \sigma_{jj}}{2} \tag{21}$$

where k_{ij} is the binary interaction parameter. In this work, k_{ij} is set to zero.

RESULTS AND DISCUSSION

Describing the PVT and phase equilibria of pure hydrocarbons, the modified PC-SAFT requires three parameters for each species, that is, m, σ, and ε/k. The parameters were obtained by minimizing the following objective function along pure n-alkane coexistence curves

$$\Omega = \sum_{j=1}^{n}\left(1 - \frac{p_{\text{cald},j}^{\text{sat}}}{p_{\text{expl},j}^{\text{sat}}}\right)^2 + \sum_{j=1}^{n}\left(1 - \frac{v_{\text{cald},j}^{\text{l}}}{v_{\text{expl},j}^{\text{l}}}\right)^2 \tag{22}$$

Table 1. Average Absolute Deviations[a] in Calculating Saturated Vapor Pressure and Saturated Liquid Volume of *n*-Alkane Series from Methane to *n*-Eicosane (for PC-SAFT-D from Propane to *n*-Eicosane)[43−50]

eq of state	saturated pressure[b]	saturated liquid volume[c]
PC-SAFT	2.33	1.08
PC-SAFT-D	2.13	1.22
this work	1.72	1.06

[a]% AAD = $(100/n)\sum_j^n$|cald − expll$_j$/expl$_j$. [b]The total number of points is 2245 (for PC-SAFT-D the total number of points is 1979). [c]The total number of points is 2584 (for PC-SAFT-D the total number of points is 2116).

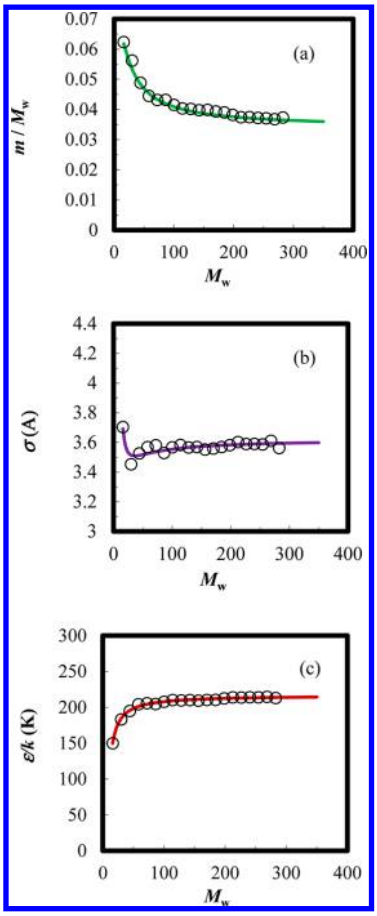

Figure 1. Correlations of pure component parameters of the new model as a function of molecular weight.

dx.doi.org/10.1021/ie400081a | Ind. Eng. Chem. Res. XXXX, XXX, XXX−XXX

Table 2. Precisions of the SAFT Approaches in Predicting the Saturated Vapor Pressures of n-$C_{22}H_{46}$, n-$C_{24}H_{50}$, and n-$C_{28}H_{58}$ (Experimental Data from Morgan and Kobayashi[51])

			% AAD[a]		
component	n	T range (K)	PC-SAFT	PC-SAFT-D	this work
n-$C_{22}H_{46}$	12	453−573	1.23	2.32	4.40
n-$C_{24}H_{50}$	12	453−588	0.48	0.98	2.15
n-$C_{28}H_{58}$	12	483−588	6.35	6.35	6.68

[a] % AAD = $(100/n)\sum_j^n |p_{sat}^{cald} - p_{sat}^{expl}|_j / p_{sat,j}^{expl}$

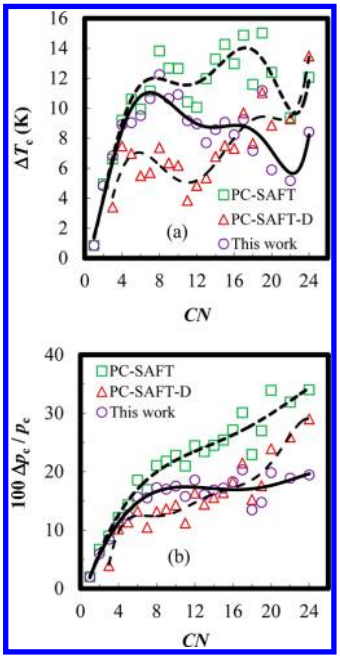

Figure 2. Deviation plots for predicting the critical temperatures [$\Delta T_c = T_{c,cald} - T_{c,expl}$] and pressures [$\Delta p_c = p_{c,cald} - p_{c,expl}$] of n-alkane series from methane to n-eicosane as a function of carbon number (experimental data from NIST Chemistry Webbook[52]).

where p^{sat} is the saturated pressure and v^l is the saturated liquid volume. For the first few n-alkanes, the PVT behavior at supercritical temperatures was also used in the fits. The pure component parameters for normal alkanes from methane to eicosane are reported in Table S1 in the Supporting Information. Also given in Table S1, the new model accurately fits the vapor pressures and saturated liquid volumes (and PVT in cases of methane to n-pentane) of short- and long-chain n-alkanes. In Table 1, the model is compared to the original PC-SAFT and PC-SAFT-D with the parameters obtained from the same sets of experimental data and eq 22 as the objective function. The fitted parameters of PC-SAFT and PC-SAFT-D are given in Tables S3 and S5 of the Supporting Information, respectively. Given in Table 1, the model outdoes PC-SAFT and PC-SAFT-D in correlating the vapor pressures and saturated liquid volumes of pure n-alkanes from methane to n-eicosane.

The model parameters behave smoothly with molecular weights as shown in Figure 1. The correlation can be represented analytically by

$$\text{parameter}\ (k) = q_{0,k} + \mathrm{M}_1 q_{1,k} + \mathrm{M}_1\mathrm{M}_2 q_{2,k} \tag{23}$$

with

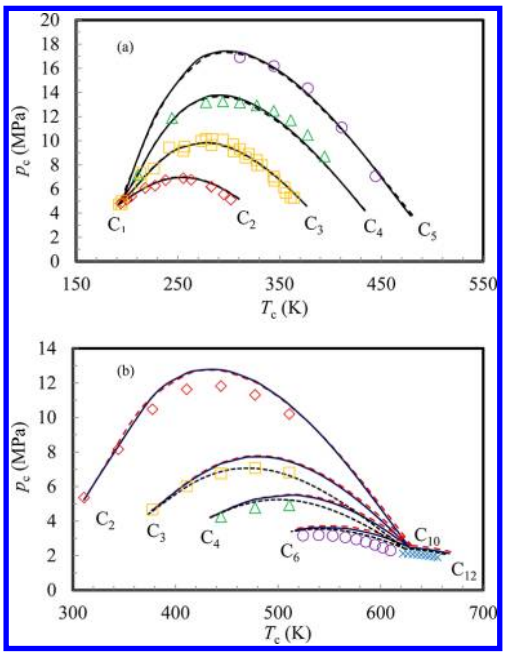

Figure 3. Critical points for binary n-alkanes systems: (a) $C_1 + C_2$, $C_1 + C_3$, $C_1 + n$-C_4, and $C_1 + n$-C_5; (b) $C_2 + n$-C_{10}, $C_3 + n$-C_{10}, n-$C_4 + n$-C_{10}, n-$C_6 + n$-C_{10}, and n-$C_{10} + n$-C_{12} (experimental data from the compilation of Hicks and Young[56]). Solid line represents this model; long dashed line, PC-SAFT; and short dashed line, PC-SAFT-D.

Table 3. Precisions of the SAFT Approaches in Predicting the Critical Points of the Systems x n-$C_9H_{20} + (1-x)$ n-$C_{13}H_{28}$ and x n-$C_{10}H_{22} + (1-x)$ n-$C_{12}H_{26}$, where x Varies from 0 to 1 and n, the Total Number of Points, Is 11 (Experimental Data from the Compilation of Hicks and Young[56])

	AAD T_c (K)[a]			% AAD p_c[b]		
system	PC-SAFT	PC-SAFT-D	this work	PC-SAFT	PC-SAFT-D	this work
n-$C_9 + n$-C_{13}	12.70	5.83	9.37	19.27	10.86	13.27
n-$C_{10} + n$-C_{12}	11.55	5.64	10.11	20.08	12.10	14.65

[a] AAD = $(1/n)\sum_j^n |T_{c,j}^{cald} - T_{c,j}^{expl}|$ [b] % AAD = $(100/n)\sum_j^n |p_{c,j}^{cald} - p_{c,j}^{expl}| / p_{c,j}^{expl}$.

$$\mathrm{M}_j = \frac{M_{W,i} - jM_{W,CH_4}}{M_{W,i}} \tag{24}$$

where parameter k can be m/M_W, σ, or ε/k and $M_{W,i}$ is the molecular weight of component i. The coefficients $q_{0,k}$, $q_{1,k}$, and $q_{2,k}$ are provided in the Supporting Information: Table S2 for the model and Tables S4 and S6 for PC-SAFT and PC-SAFT-D, respectively. One of the features of eq 23 is that the equation can also be used to extrapolate the model parameters to chain molecules longer than n-eicosane. Given in Table 2, the new model, PC-SAFT, and PC-SAFT-D with eq 23 were used to predict the vapor pressures of n-docosane, n-tetracosane, and n-octacosane. The agreements with experimental data were good for the three equations of state. PC-SAFT surpasses the two others, however.

Because SAFT and its derivatives are based on a mean field theory, significant disagreement is expected at or near the vapor−liquid critical points. The new model, which takes advantage of a dimer theory, however, provides improvement compared to PC-SAFT. As shown in Figure 2, the improve-

dx.doi.org/10.1021/ie400081a | Ind. Eng. Chem. Res. XXXX, XXX, XXX−XXX

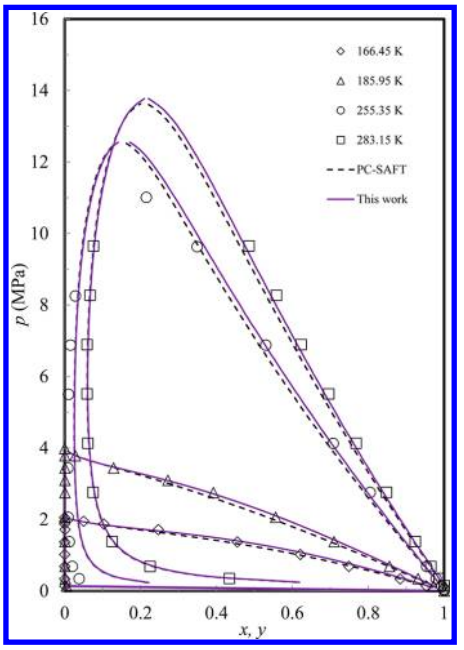

Figure 4. VLE of the system $(1 - x)$ C_1 + x n-C_4 (experimental data from Kahre[57]).

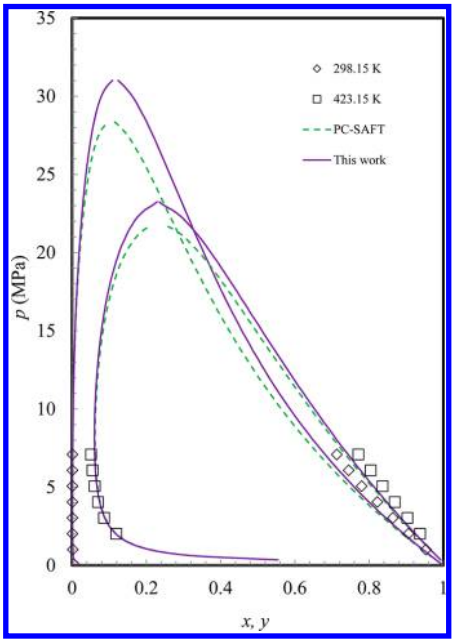

Figure 5. VLE of the system $(1 - x)$ C_1 + x n-C_8 (experimental data from Kohn and Bradish[58]).

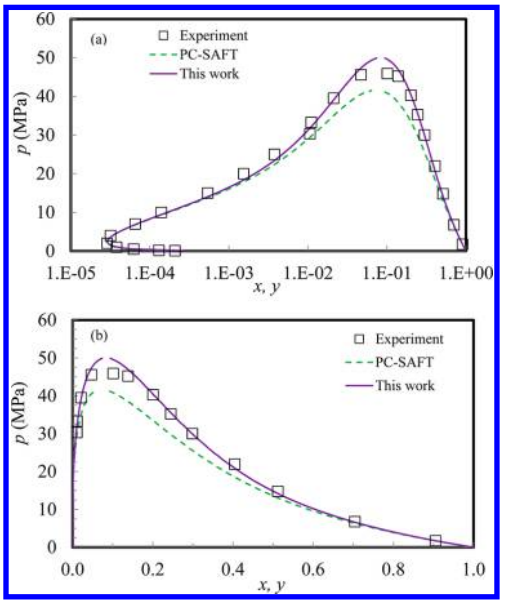

Figure 6. VLE of the system $(1 - x)$ C_1 + x n-C_{12} at 303.15 K (experimental data from Rijkers et al.[59]) at two different compositional ranges.

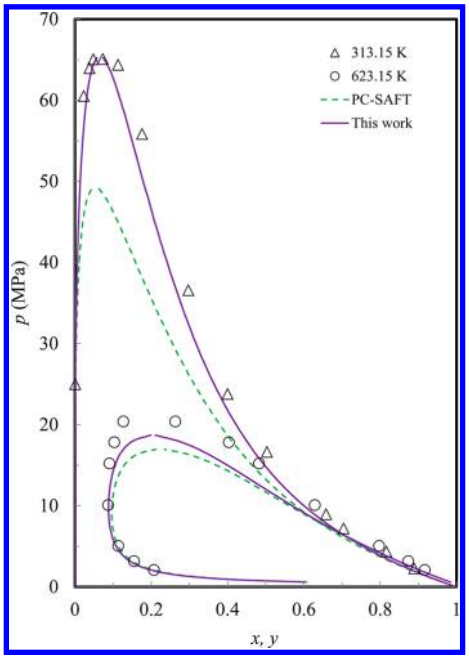

Figure 7. VLE of the system $(1 - x)$ C_1 + x n-C_{16} (experimental data from Rijkers et al.[60] and Lin et al.[61]).

ment starts from n-butane toward longer n-alkanes. For comparison, the critical points predicted by PC-SAFT-D from propane to n-tetracosane were also included. Interestingly, PC-SAFT-D is more accurate than the new model up to n-hexadecane. Afterward, the model overtakes PC-SAFT-D. The high accuracy of PC-SAFT-D can be attributed to rescaling 21 of 42 universal constants of the dispersion term in PC-SAFT-D. It is worth noting that Gross and Sadowski[25] developed the PC-SAFT approach by providing a dispersion term with 42 universal constants. In obtaining these constants, the saturated properties and PVT of the first eight n-alkanes were also included in the regression process. Consequently, PC-SAFT improved the SAFT approach of Huang and Radosz,[11,12] especially near the critical points.[6,25] Following Gross and Sadowski,[25] Dominik et al.[27] rescaled 21 of 42 universal constants of the PC-SAFT dispersion term by including the saturated and PVT properties of propane to n-decane. Although including experimental critical points during the regression is not expressed by the authors, PC-SAFT-D accurately predicts the critical points of n-alkanes, especially the first 10 hydrocarbons.

In Figure 3a, the model is compared to PC-SAFT for predicting[53−55] the vapor−liquid critical points of n-alkane systems containing methane. No clear improvement is seen in Figure 3a. For methane, the model clearly reduces to PC-SAFT. For ethane, propane, and n-butane, the model does not offer

dx.doi.org/10.1021/ie400081a | Ind. Eng. Chem. Res. XXXX, XXX, XXX−XXX

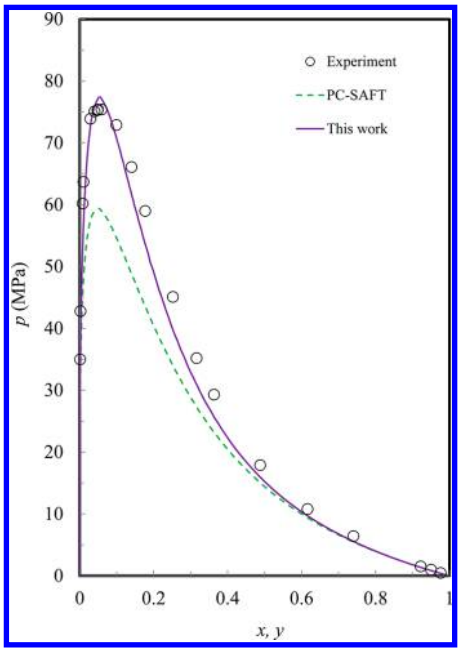

Figure 8. VLE of the system $(1 - x)$ C_1 + x n-C_{20} at 353.15 K (experimental data from van der Kooi et al.[62]).

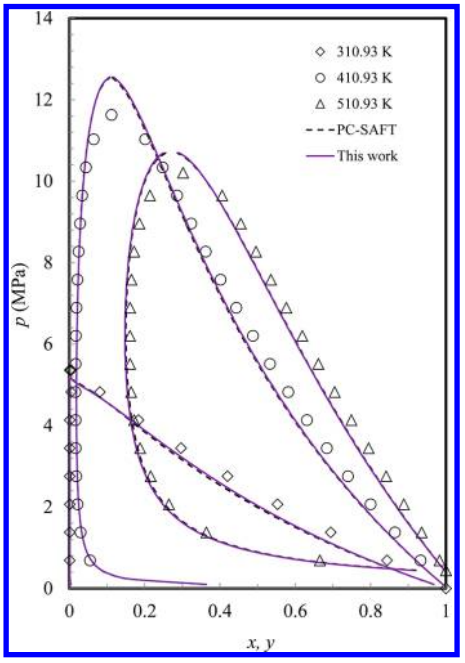

Figure 9. VLE of the system $(1 - x)$ C_2 + x n-C_{10} (experimental data from Reamer and Sage[63]).

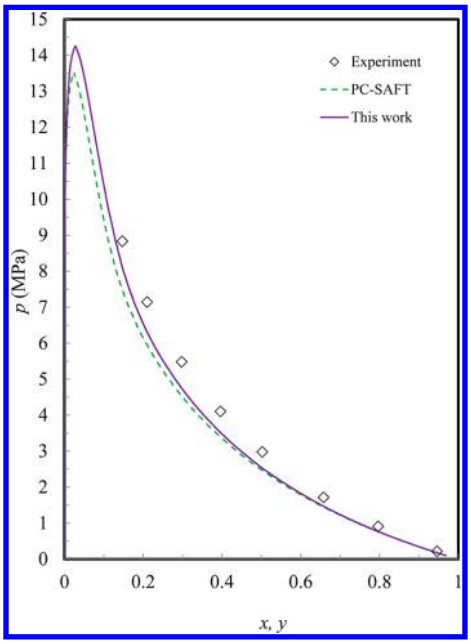

Figure 10. VLE of the system $(1 - x)$ C_2 + x n-C_{22} at 340 K (experimental data from Peters at al.[64]).

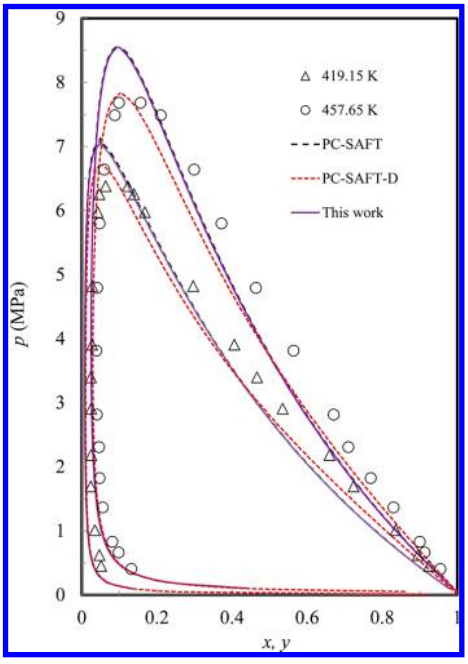

Figure 11. VLE of the system $(1 - x)$ C_3 + x n-C_{22} (experimental data from Gardeler et al.[65]).

any headway in predicting the critical points as shown in Figure 2. Therefore, it can be expected that the model identically predicts the critical points with PC-SAFT. In Figure 3b, both the new model and PC-SAFT describe reasonably the critical points of the binary mixtures containing *n*-decane with other *n*-alkanes. Predictions from PC-SAFT-D were also included for comparisons. Clearly, PC-SAFT-D is more accurate, especially for the system propane + *n*-decane. The differences can be marked in Table 3, where the predicted critical temperatures and pressures of two binary systems, n-C_9H_{20} + n-$C_{13}H_{28}$ and n-$C_{10}H_{22}$ + n-$C_{12}H_{26}$, are compared to the experimental data. Clearly, for mixtures of long *n*-alkanes, the new model performs well and better than PC-SAFT. PC-SAFT-D is more accurate than both equations, however.

The VLE of the systems methane + *n*-butane and methane + *n*-octane are shown in Figures 4 and 5, respectively. The model and PC-SAFT are clearly identical for methane. Then, the effect of chain on the phase behavior goes through the longer *n*-alkane. As shown in Figure 2, however, the chain effect is only perceptible for hydrocarbons heavier than *n*-butane. It then explains the fact that the model and PC-SAFT identically predicted the VLE of the system methane + *n*-butane. No marked difference is seen, especially near the critical point. In Figure 5, the model and PC-SAFT predicted (k_{ij} = 0) well the

dx.doi.org/10.1021/ie400081a | Ind. Eng. Chem. Res. XXXX, XXX, XXX−XXX

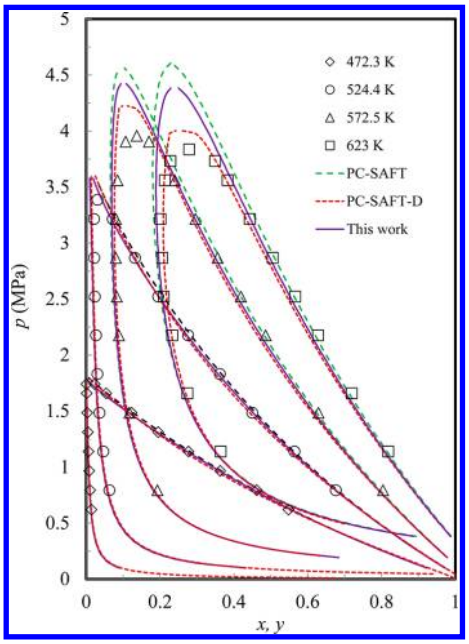

Figure 12. VLE of the system $(1 - x)$ C_6 + x n-C_{16} (experimental data from Joyce and Thies[66]).

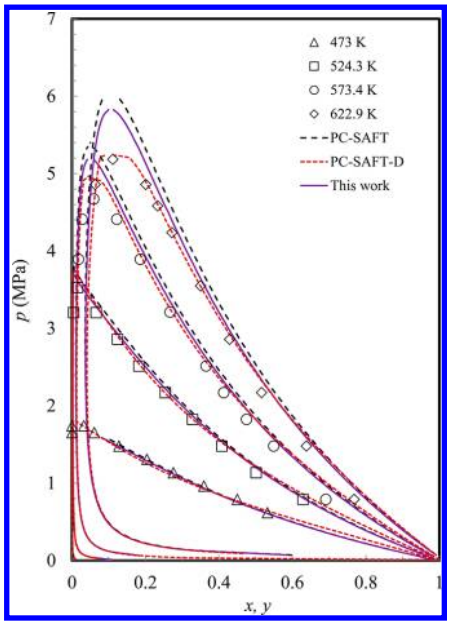

Figure 13. VLE of the system $(1 - x)$ C_6 + x n-C_{24} (experimental data from Joyce et al.[67]).

experimental values, although the differences are marked toward the critical points. Figures 6−8 show that the new model accurately predicted the VLE of the systems methane + *n*-dodecane, methane + *n*-hexadecane, and methane + *n*-eicosane far from and near the critical points. However, PC-SAFT fails near the critical points. That can be explained again in terms of chain length for the longer *n*-alkanes. As shown in Figure 2, the longer the hydrocarbon, the more accurate the representation of the model compared to PC-SAFT at the critical point. The accuracy at the critical points improved the model behavior near the critical point. Because no binary interaction parameter was used, the improvement is adequate.

For binary systems containing ethane and long-chain hydrocarbons, the difference in the performance of the new

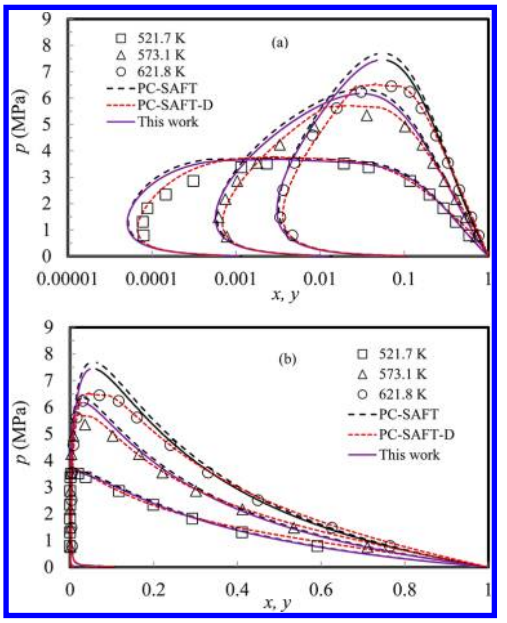

Figure 14. VLE of the system $(1 - x)$ C_6 + x n-C_{36} (experimental data from Joyce et al.[67]).

model and PC-SAFT is less clear compared to the binary systems containing methane. In Figure 9, where the VLE of ethane + *n*-decane are shown, the differences are not profound. Figure 10, however, shows marked differences between the two models in predicting the VLE of ethane + *n*-docosane. Clearly, the new model is more accurate. Comparisons in Figures 9 and 10 clarify that in addition to chain length in binary *n*-alkane mixtures, the size ratio of the two hydrocarbons also matters in the VLE of the system.[6] For instance, the size ratio of *n*-decane to ethane is close to the size ratio of *n*-butane to methane. Consequently, both model and PC-SAFT identically predicted the VLE of the two systems.

Shown in Figure 11, the performances of the new model and PC-SAFT are clearly equal in predicting the VLE of the system propane + *n*-docosane. Because PC-SAFT-D is also applicable to systems with hydrocarbons longer than propane, Figure 11 also includes the VLE of the system according to PC-SAFT-D. Clearly, PC-SAFT-D significantly describes the VLE of the system near the critical points, whereas no precaution for density fluctuations near the critical point was deemed. That could be a direct consequence of rescaling the dispersion term universal constants.

The three models were also compared to predict the VLE of the binary systems *n*-hexane + *n*-hexadecane and *n*-hexane + *n*-tetracosane, respectively. The three models are in good agreement with experimental data far from the critical points as shown in Figures 12 and 13. Toward the critical points, however, PC-SAFT-D performs clearly better than both. In Figure 14, the VLE of the system *n*-hexane + *n*-hexatriacontane are depicted. Again, PC-SAFT-D exceeds the two other models near the critical point. Away from the critical point, it slightly overpredicts the dew point curve at high temperatures and bubble point curve for all temperatures.

■ CONCLUSIONS

A simplified hard-chain dimer theory has been used to modify the PC-SAFT equation of state. The new model has calculated accurately the saturated pressures and liquid volumes of pure *n*-

dx.doi.org/10.1021/ie400081a | Ind. Eng. Chem. Res. XXXX, XXX, XXX−XXX

alkanes. Starting from *n*-butane, the model has calculated the pure component critical pressures and temperatures of *n*-alkanes more accurately than PC-SAFT. For the VLE of binary *n*-alkane systems, the model has performed more accurately than PC-SAFT near critical points for systems with a size ratio larger than 4. For other systems, the model and PC-SAFT are identical. Whereas no binary interaction parameter has been used, the new model has adequately described the VLE of binary *n*-alkane systems, in particular, systems containing methane and a long-chain *n*-alkane. In systems containing ethane, propane, or *n*-hexane and a long-chain hydrocarbon, the performances of the new model and PC-SAFT have almost been identical with the exception of near the critical points, where the new model shows superiority.

■ ASSOCIATED CONTENT

Supporting Information

Parameters of the model, PC-SAFT, and PC-SAFT-D. This material is available free of charge via the Internet at http://pubs.acs.org.

■ AUTHOR INFORMATION

Corresponding Author

*Phone: +6019 528 9780. Fax: +6005 365 6167. E-mail: khashayar_nasrifar@petronas.com.my.

Notes

The authors declare no competing financial interest.

■ SYMBOLS

a = reduced Helmholtz free energy (A/RT)
a_j = polynomial given by eq 18
a_{0i}, a_{1i}, a_{2i} = coefficients provided by ref 25
A = molar Helmholtz free energy (J mol^{-1})
b_j = polynomial given by eq 19
b_{0i}, b_{1i}, b_{2i} = coefficients provided by ref 25
C_1 = compressibility of a hard-chain fluid given by eq 15
d = soft repulsion diameter (m)
g = radial distribution function at contact
I_1 = abbreviation defined by eq 16
I_2 = abbreviation defined by eq 17
k = Boltzmann constant (1.38066×10^{-23} J K^{-1})
k_{ij} = binary interaction parameter
m = number of segments in a molecule
$\bar{m}$ = mean value for the number of segments in a mixture
M_{Wi} = molecular weight of component i
n = number of experimental data points
p = pressure (MPa)
$q_{0,k}$, $q_{1,k}$, $q_{2,k}$ = coefficients provided in Tables S2, S4, and S6 of the Supporting Information for different equations of state
R = universal gas constant (8.314 J mol^{-1} K^{-1})
S_R = ratio of surface area for a hard-dimer to a hard-sphere with the same volume as the hard-dimer
T = temperature (K)
v = liquid volume (m^3 kmol^{-1})
x = mole fraction
Z = compressibility factor

Greek Letters

ε = depth of square-well potential (J)
ζ = parameter defined by eq 6
η = packing fraction (ζ_3)
$\delta = (1 + 2^{1/3})/2 \approx 1.12996$
M = reduced molecular weight defined by eq 24
π = constant (3.1415926)
ρ = number density (m^{-3})
σ = diameter of a segment (Å)
Ω = objective function

Subscripts/Superscripts

assoc = association
calc = calculated value
chain = chain term
disp = dispersion
expl = experimental value
hc = hard-chain
hd = hard-dimer
hs = hard-sphere
i, j, k = dummy indices
l = liquid
n = dummy index
polar = polar term
res = residual
sat = saturated

■ REFERENCES

(1) Flöter, E. *Hyperbaric Reservoir Fluids Phase Behaviour of Model Systems*. Ph.D. Dissertation, Technical University of Delft, Delft, The Netherlands, 1999.

(2) Flöter, E.; de Loos, Th. W.; de Swaan Arons, J. Improved Modeling of the Phase Behaviour of Asymmetric Hydrocarbon Mixtures with the Peng-Robinson Equation of State Using a Different Temperature Dependency of the Parameter *a*. *Ind. Eng. Chem. Res.* **1998**, *37*, 1651.

(3) Farshchi Tabrizi, F.; Nasrifar, Kh. Application of Predictive Equations of State in Calculating Natural Gas Phase Envelopes and Critical Points. *J. Nat. Gas. Sci. Eng.* **2010**, *2*, 21.

(4) Peters, C. J.; de Swaan Arons, J.; Sengers, J. M. H. L.; Gallagher, J. S. Global Phase Behaviour of Mixtures of Short and Long *n*-Alkanes. *AIChE J.* **1988**, *34*, 834.

(5) Ting, P. D.; Joyce, P. C.; Jog, P. K.; Chapman, W. G.; Thies, M. C. Phase Equilibrium Modeling of Long-Chain and Short-Chain Alkanes Using Peng-Robinson and SAFT. *Fluid Phase Equilib.* **2003**, *30*, 267.

(6) Aparicio-Martínez, S.; Hall, K. R. Use of PC-SAFT for Global Phase Diagrams in Binary Mixtures Relevant to Natural Gases. 1. *n*-Alkane + *n*-Alkane. *Ind. Eng. Chem. Res.* **2007**, *46*, 273.

(7) Chapman, W. G.; Jackson, G.; Gubbins, K. E. Phase Equilibria of Associating Fluids. Chain Molecules with Multiple Bonding Sites. *Mol. Phys.* **1988**, *65*, 1057.

(8) Chapman, W. G.; Gubbins, K. E.; Jackson, G.; Radosz, M. New Reference Equation of State for Associating Liquids. *Ind. Eng. Chem. Res.* **1990**, *29*, 1709.

(9) Von Solms, N.; Kouskoumverkaki, I. A.; Michelsen, M. L.; Kontogeorgis, G. M. Capabilities, Limitations and Challenges of a Simplified PC-SAFT Equation of State. *Fluid Phase Equilib.* **2006**, *241*, 344.

(10) Tihic, A.; Von Solms, N.; Michelsen, M. L.; Kontogeorgis, G. M. Application of sPC-SAFT and Group Contribution sPC-SAFT to Polymer Systems − Capabilities and Limitations. *Fluid Phase Equilib.* **2009**, *281*, 70.

(11) Huang, S. H.; Radosz, M. Equation of State for Small, Large, Polydisperse, and Associating Molecules. *Ind. Eng. Chem. Res.* **1990**, *29*, 2284.

(12) Huang, S. H.; Radosz, M. Equation of State for Small, Large, Polydisperse, and Associating Molecules: Extension to Fluid Mixtures. *Ind. Eng. Chem. Res.* **1991**, *30*, 1994.

(13) Blas, F. J.; Vega, L. F. Thermodynamic Behaviour of Homonuclear and Hetronuclear Lennard-Jones Chains with Association Sites from Simulation and Theory. *Mol. Phys.* **1997**, *92*, 135.

(14) Blas, F. J.; Vega, L. F. Prediction of Binary and Ternary Diagrams Using the Statistical Associating Fluid Theory (SAFT) Equation of State. *Ind. Eng. Chem. Res.* **1998**, *37*, 660.
(15) Pámies, J. C.; Vega, L. F. Vapor−Liquid Equilibria and Critical Behaviour of Heavy *n*-Alkane Using Transferable Parameters from the Soft-SAFT Equation of State. *Ind. Eng. Chem. Res.* **2001**, *40*, 2532.
(16) Llovell, F.; Vega, L. F. Phase Equilibria, Critical Behaviour and Derivative Properties of Selected *n*-Alkane/*n*-Alkane and *n*-Alkane/1-Alkanol Mixtures by the Crossover Soft-SAFT Equation of State. *J. Supercrit. Fluids* **2007**, *41*, 204.
(17) White, J. A. Contribution of Fluctuation to Thermal Properties of Fluids with Attractive Potential Force of Limited Range: Theory Compared with $P\rho T$ and C_v Data for Argon. *Fluid Phase Equilib.* **1992**, *75*, 53.
(18) Salvino, L. W.; White, J. A. Calculation of Density Fluctuation Contributions of Thermodynamic Properties of Simple Fluids. *J. Chem. Phys.* **1992**, *96*, 4559.
(19) Gil-Villegas, A.; Galindo, A.; Whitehead, P. J.; Mills, S. L.; Jackson, G.; Burguess, A. N. Statistical Association Fluid Theory for Chain Molecules with Attractive Potentials of Variable Range. *J. Chem. Phys.* **1997**, *106*, 4168.
(20) McCabe, C.; Galindo, A.; Gil-Villegas, A.; Jackson, G. Predicting the High-Pressure Phase Equilibira of Binary Mixtures of *n*-Alkanes Using the SAFT-VR Approach. *Int. J. Thermophys.* **1998**, *19*, 1511.
(21) Sun, L.; Zhao, H.; Kiselev, S. B.; McCabe, C. Application of SAFT-VRX to Binary Phase Behaviour: Alkanes. *Fluid Phase Equilib.* **2005**, *228−229*, 275.
(22) Kiselev, S. B. Cubic Crossover Equation of State. *Fluid Phase Equilib.* **1998**, *147*, 7.
(23) Kiselev, S. B.; Friend, D. G. Cubic Crossover Equation of State for Mixtures. *Fluid Phase Equilib.* **1999**, *162*, 51.
(24) Gross, J.; Sadowski, G. Application of Perturbation Theory to a Hard-Chain Reference Fluid: An Equation of State for Square-Well Chains. *Fluid Phase Equilib.* **2000**, *168*, 183.
(25) Gross, J.; Sadowski, G. Perturbed-Chain SAFT: An Equation of State Based on a Perturbation Theory for Chain Molecules. *Ind. Eng. Chem. Res.* **2001**, *40*, 1244.
(26) Wertheim, M. S. Thermodynamic Perturbation Theory of Polymerization. *J. Chem. Phys.* **1987**, *87*, 7323.
(27) Dominik, A.; Jain, S.; Chapman, W. G. New Equation of State for Polymer Solutions Based on the Statistical Associating Fluid Theory (SAFT) − Dimer Equation for Hard-Chain Molecules. *Ind. Eng. Chem. Res.* **2007**, *46*, 5766.
(28) Ghonasgi, D.; Chapman, W. G. A New Equation of State for Chain Molecules. *J. Chem. Phys.* **1994**, *100*, 6633.
(29) Chang, J.; Sandler, S. I. An Equation of State for the Hard-Sphere Chain Fluid: Theory and Monte Carlo. *Chem. Eng. Sci.* **1994**, *49*, 2777.
(30) Nasrifar, Kh.; Bolland, O. Simplified Hard-Sphere and Hard-Sphere Chain Equations of State for Engineering Applications. *Chem. Eng. Commun.* **2006**, *193*, 1277.
(31) Nasrifar, Kh. A Semi-Empirical Hard-Sphere Chain Equation of State: Pure and Mixture. *Fluid Phase Equilib.* **2007**, *261*, 258.
(32) Müller, E. A.; Gubbins, K. E. Molecular-Based Equations of State for Associating Fluids: Review of SAFT and Related Approaches. *Ind. Eng. Chem. Res.* **2001**, *40*, 2193.
(33) Tafazzol, A. H.; Nasrifar, Kh. Thermophysical Properties of Associating Fluids in Natural Gas Industry Using PC-SAFT Equation of State. *Chem. Eng. Commun.* **2011**, *198*, 1244.
(34) Nasrifar, Kh.; Tafazzol, A. H. Vapor−Liquid Equilibria of Acid Gas−Aqueous Ethanolamine Solutions Using the PC-SAFT Equation of State. *Ind. Eng. Chem. Res.* **2010**, *49*, 7620.
(35) Tumakara, F.; Sadowski, G. Application of the Perturbed-Chain SAFT Equation State to Polar Systems. *Fluid Phase Equilib.* **2004**, *217*, 233.
(36) Karakatsani, E. K.; Economou, I. G. Phase Equilibrium Calculations for Multi-Component Polar Fluid Mixtures with tPC-PSAFT. *Fluid Phase Equilib.* **2007**, *261*, 265.
(37) Dominik, A.; Chapman, W. G.; Kleinee, M.; Sadowski, G. Modeling of Polar Systems with the Perturbed-Chain SAFT Equation of State. Investigation of the Performance of Two Polar Terms. *Ind. Eng. Chem. Res.* **2005**, *44*, 6928.
(38) Tumakaka, F.; Gross, J.; Sadowski, G. Thermodynamic Modeling of Complex Systems Using PC-SAFT. *Fluid Phase Equilib.* **2005**, *228−229*, 89.
(39) Karakatsani, E. K.; Economou, I. G. Perturbed Chain-Statistical Associating Fluid Theory Extended to Dipolar and Quadrupolar Molecular Fluids. *J. Phys. Chem. B* **2006**, *110*, 9252.
(40) Boublik, T. Hard Sphere Equation of State. *J. Chem. Phys.* **1970**, *53*, 471.
(41) Mansoori, G. A.; Carnahan, N. F.; Starling, K. E.; Leland, T. W. Equilibrium Thermodynamic Properties of the Mixture of Hard Spheres. *J. Chem. Phys.* **1971**, *54*, 1523.
(42) Barker, J. A.; Henderson, D. Perturbation Theory and Equation of State for Fluids. I. The Square Well Potential. *J. Chem. Phys.* **1967**, *47*, 4714.
(43) Vargaftik, N. B.; Vinogradov, Y. K.; Yargin, V. S. *Handbook of Physical Properties of Liquids and Gases (Pure Substance and Mixtures)*; Begell House: New York, 1996.
(44) Daubert, T. E., Danner, R. P.; Sibul, H. M.; Stebbin, C. C. *DIPPR Data Compilation of Pure Compound Properties*; Design Institute for Physical Property Data, AIChE: New York, 1993.
(45) Wagner, W.; de Reuck, K. M. *Methane. International Thermodynamic Tables of the Fluid State*; IUPAC, Blackwell: Oxford, U.K., 1996; Vol. 3.
(46) Beattie, J. A.; Simard, G. A.; Su, G.-J. The Compressibility of and an Equation of State for Gaseous Normal Butane. *J. Am. Chem. Soc.* **1939**, *61*, 26.
(47) Beattie, J. A.; Levine, S. W.; Douslin, D. R. The Compressibility of and an Equation of State for Gaseous Normal Pentane. *J. Am. Chem. Soc.* **1952**, *74*, 4778.
(48) Kelso, E. A.; Felsing, W. A. The Pressure−Volume−Temperature Relations of *n*-Hexane and of 2-Methylpentane. *J. Am. Chem. Soc.* **1940**, *62*, 3132.
(49) Vargaftik, N. B. *Tables of Thermodynamic Properties of Liquids and Gases*; Wiley: New York, 1975.
(50) ASHRAE, American Society of Heating and Refrigeration and Air Conditioning Engineer, New York, 1989.
(51) Morgan, D. L.; Kobayashi, R. Direct Vapor Pressure Measurements of Ten *n*-Alkanes in the C10−C28 Range. *Fluid Phase Equilib.* **1994**, *97*, 211.
(52) NIST Chemistry Webbook, available at http://webbook.nist.gov/chemistry/.
(53) Justo-García, D. N.; García-Sanchez, F.; Díaz-Ramírez, N. L.; Romero-Martínez, A. Calculation of Critical Points for Multicomponent Mixtures Containing Hydrocarbon and Nonhydrocarbon Components with the PC-SAFT Equation of State. *Fluid Phase Equilib.* **2008**, *265*, 192.
(54) Heidmann, R. A.; Khalil, A. M. The Calculation of Critical Points. *AIChE J.* **1980**, *26*, 769.
(55) Arce, P.; Aznar, M. A. Modeling of Critical Lines and Regions for Binary and Ternary Mixtures Using Non-Cubic and Cubic Equations of State. *J. Supercrit. Fluid* **2007**, *42*, 1.
(56) Hicks, C. P.; Young, C. L. The Gas-Liquid Critical Properties of Binary Mixtures. *Chem. Rev.* **1975**, *75*, 119.
(57) Kahre, L. C. Low-Temperature *K* Data for Methane−Butane. *J. Chem. Eng. Data* **1974**, *19*, 67.
(58) Kohn, J. P.; Bradish, W. F. Multiphase and Volumetric Equilibria of the Methane−*n*-Octane System at Temperatures between −100° and 150°. *J. Chem. Eng. Data* **1964**, *9*, 5.
(59) Rijkers, M. P. W. M.; Maduro, V. B.; Peters, C. J.; de Swaan Arons, J. Measurements on the Phase Behaviour of Binary Mixtures for Modeling the Condensation Behaviour of Natural Gas: Part II. The System Methane + Dodecane. *Fluid Phase Equilib.* **1992**, *72*, 309.
(60) Rijkers, M. P. W. M.; Peters, C. J.; de Swaan Arons, J. Measurements on the Phase Behaviour of Binary Mixtures for

Modeling the Condensation Behaviour of Natural Gas: Part III. The System Methane + Hexadecane. *Fluid Phase Equilib.* **1993**, *85*, 335.
(61) Lin, H.-M.; Sebastian, H. M.; Chao, K.-C. Gas−Liquid Equilibrium in Hydrogen + *n*-Hexadecane and methane + *n*-Hexadecane at Elevated Temperatures and Pressures. *J. Chem. Eng. Data* **1980**, *25*, 252.
(62) Van der Kooi, H. J.; Flöter, E.; de Loos, Th. W. High-Pressure Phase Equilibria of $\{(1 - x)\ CH_4 + x\ CH_3\ (CH_2)_{18}\ CH_3\}$. *J. Chem. Eng. Thermodyn.* **1995**, *27*, 847.
(63) Reamer, H. H.; Sage, B. H. Phase Equilibria in Hydrocarbon Systems. Volumetric and Phase Behavior of the Ethane−*n*-Decane System. *J. Chem. Eng. Data* **1962**, *7*, 161.
(64) Peters, C. J.; Spiegelaar, J.; de Swaan Arons, J. Phase Equilibria in Binary Mixtures of Ethane + Docosane and Molar Volumes of Liquid Docosane. *Fluid Phase Equilib.* **1988**, *41*, 245.
(65) Gardeler, H.; Fischer, K.; Gmehling, J. Experimental Determination of Vapor-Liquid Equilibrium Data for Asymmetric Systems. *Ind. Eng. Chem. Res.* **2002**, *41*, 1051.
(66) Joyce, P. C.; Thies, M. C. Vapor−Liquid Equilibrium for the Hexane + Hexadecane and Hexane + 1- Hexadecanol System at Elevated Temperatures and Pressures. *J. Chem. Eng. Data* **1998**, *43*, 819.
(67) Joyce, P. C.; Gordon, J.; Theis, M. C. Vapor−Liquid Equilibria for Hexane + Tetracosane and Hexane + Hexatriacontane at Elevated Temperatures and Pressures. *J. Chem. Eng. Data* **2000**, *45*, 424.